

CFD ANALYSIS ON THE EQUATIONS OF SUBMARINE STERN SHAPE

*M. Moonesun**[†] *Y.M. Korol*** and *A. Brazhko****

* Maleke-ashtar University of Technology, Faculty of Ship Design, Researcher in hydrodynamics of submersibles

** National University of Shipbuilding Admiral Makarov (NUOS), Faculty of Ship Design, Professor, Ukraine

*** National University of Shipbuilding Admiral Makarov (NUOS), Faculty of Ship Design, PhD, Ukraine

Keywords: Submarine, Hydrodynamic, Equation, Resistance, Optimum, Shape, Stern

ABSTRACT

This paper discusses about an optimum hydrodynamic shape of stern of submarine in minimum resistance point of view. Submarines have two major categories for hydrodynamic shape: tear drop shape and cylindrical middle body shape. Here, submarine with parallel (cylindrical) middle body are studied because, the most of naval submarines and ROVs have cylindrical middle body shape. Every hull shape, have three parts: bow, cylinder and stern. This paper wants to propose an optimum stern shape by CFD method and Flow Vision software. Major parameter in hydrodynamic design of stern is wake field (variation of fluid velocity) and resistance. The focus of this paper is on the resistance at fully submerge mode without free surface effects.

Firstly, all available equations for the stern shape of submarine are presented. Secondly, for all equations of shapes, CFD analysis has been done. In all models, the velocity, dimensions of domain, diameter, bow shape and the total length (bow, middle and stern length) are constant.

INTRODUCTION

Every hull shape of submarine has four parts: bow, cylinder, stern and sail [1]. These parts have important roles in submarine hydrodynamic that can be designed in several different cases [2]. Fig.1 shows a sample for submarine shape and its dimension relations [3]. Submarines are encountered to limited energy in submerged navigation and because of that, the minimum resistance is vital in submarine hydrodynamic design. Technical discussions about submarine hydrodynamic design were done in Ref. books [4-11] and Ref. papers [12-20]. Stern of submarine, plays some roles in submarine hydrodynamic design such as wake field (variation of fluid velocity) and resistance. The focus of this paper is on the resistance at fully submerge mode without free surface effects.

In addition to the hydrodynamic, the shape of stern, depends on the internal architecture and general arrangements of the stern part. Figure 2 shows a usual internal arrangement inside the stern of submarine that limits the

shape of stern. Related materials about general arrangement in naval submarines are presented in [4-7,18] and discussions about general shape of submarines, there are in [21-24]. The hull structure of submarine has two main category: pressure hull and light hull. Pressure hull, provides a dry space in atmospheric pressure for human life, electric and other devices that are sensitive to the humidity and high pressures. Light hull, provides a wetted space for the devices which can sustain the pressure of the depth of the ocean. According to Fig.2, stern part, being composed of pressure hull (end compartment) and light hull. The slope of the stern shape should be acceptable for arranging all equipment with reasonable clearance for accessibility and repairing. The most part of the stern is occupied by main ballast tank (MBT) which needs a huge volume inside the stern. The more length of stern is equal to the better hydrodynamic conditions, and worse condition for the length of the motor shaft. There are several suggestions for the stern length such as IHSS and [3], but

[†] Corresponding author(m.moonesun@gmail.com)

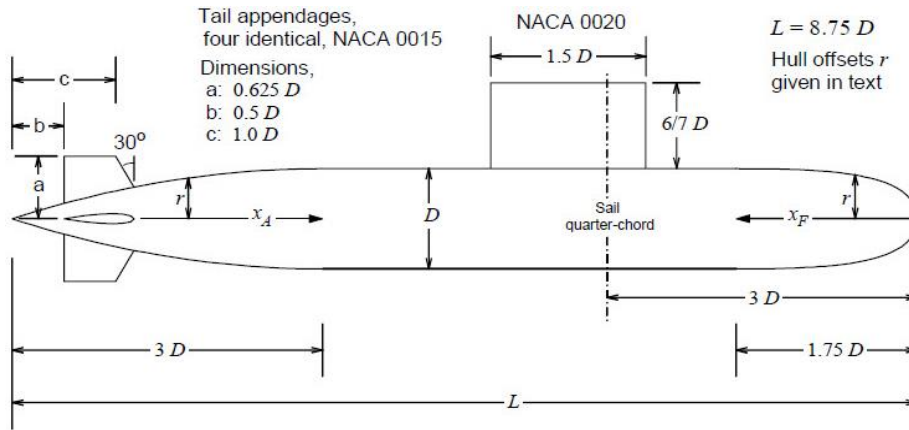


Fig. 1 A sample for the dimensions of submarine hull [3]

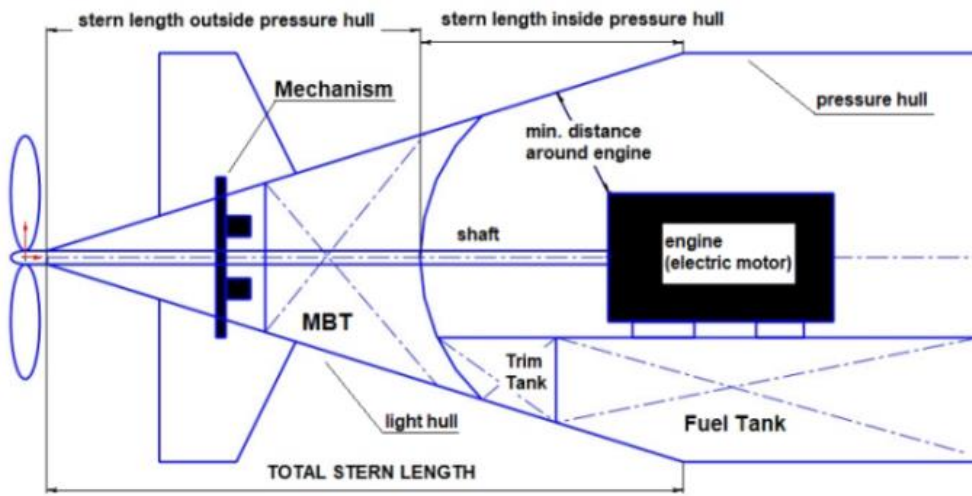


Fig. 2 General arrangement of stern part (inside and outside of the pressure hull)

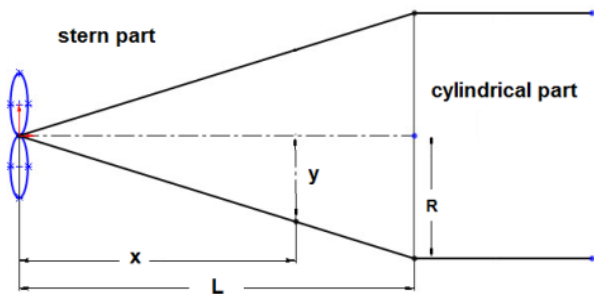


Fig. 3 Reference coordinate and parameters

another important subject, is the curvature and the shape of the stern specially in the light hull part. The focus of this paper is on the curvature and the shape equation of the stern. Submarines have two major categories for hydrodynamic shape: tear drop shape and cylindrical middle body shape. This paper wants to reply to this question because, the most real and naval submarines and ROV's have cylindrical middle body shape, for example, in IHSS series [25].

Submarines have two modes of navigation: surfaced mode and submerged mode. In surfaced mode of navigation, the energy source limitation is lesser than the submerged mode. Therefore, in really naval submarines, the base state of determination of required power of propulsion engines is the submerged mode. The focus of this paper is on resistance at fully submerge mode without free surface effects. This paper is a part of scientific researches in the program of Iranian Hydrodynamic Series of Submarines (IHSS).

GENERAL SHAPES FOR THE STERN

Reference coordinate and parameters

Reference coordinate and parameters are shown in Fig. 3. The full body of revolution of the stern is formed by rotating the profile around the centerline (CL). Note that the equations describe the 'perfect' shape meanwhile, in practice, the end of stern is often blunted or truncated for manufacturing or installing the shaft and propeller (as

shown in Fig.2). The equations of curvatures are presented in [26,27].

a) Conical: This shape is very usual and common stern in submarines. This shape is often chosen for its ease of manufacture, and is also a bad selection for its resistance characteristics. The sides of a conical profile are straight lines, so the diameter equation is simply: $y = x \cdot R/L$. Cones are sometimes defined by their half angle, ϕ (Fig.4-a):

$$\phi = \arctan \frac{R}{L} \quad \text{and} \quad y = x \cdot \tan \phi$$

b) Spherically blunted cone: In most applications, a conical stern is often blunted by capping it with a segment of a sphere or cut vertically because the shaft exit, bearings and couplings, needs some distance before the end of cone (Fig.4-b). The tangency point where the sphere meets the cone can be found from:

$$x_t = \frac{L^2}{R} \sqrt{\frac{r_n^2}{R^2 + L^2}} \quad y_t = \frac{x_t R}{L}$$

r_n is the radius of the spherical nose cap. The center of the spherical nose cap can be found from:

$$x_0 = x_t + \sqrt{r_n^2 - y_t^2}$$

$$x_a = x_0 - r_n$$

c) Bi-conic: This stern includes from two cones with different slope with length and radius of L_1, R_1, L_2, R_2 and thus: $L = L_1 + L_2$ (Fig.4-c) :

$$0 \leq x \leq L_1 : y = \frac{x \cdot R_1}{L_1}, \quad \phi_1 = \arctan \frac{R_1}{L_1} \quad \text{and}$$

$$y = x \cdot \tan \phi_1$$

$$L_1 \leq x \leq L : y = R_1 + \frac{(x - L_1)(R_2 - R_1)}{L_2},$$

$$\phi_2 = \arctan \frac{R_2 - R_1}{L_2} \quad \text{and} \quad y = R_1 + (x - L_1) \tan \phi_2,$$

d) Tangent ogive: The profile of this shape is formed by a segment of a circle such that the body is tangent to the curve of the stern at its base; and the base is on the radius of the circle (Fig.4-d). The popularity of this shape is largely due to the ease of constructing its profile. The radius of the circle that forms the ogive is called the ogive radius, ρ , and it is related to the length and base radius of the stern as expressed by the formula: $\rho = (R^2 + L^2) / 2R$

The radius y at any point x , as x varies from 0 to L is:

$$y = \sqrt{\rho^2 - (L - x)^2} + R - \rho$$

The stern length, L , must be less than or equal to ρ . If they are equal, then the shape is a hemisphere.

e) Spherically blunted tangent ogive: According to Fig4-e, a tangent ogive stern is often blunted by capping it with a segment of a sphere. The tangency point where the sphere meets the tangent ogive can be found from:

$$x_0 = L - \sqrt{(\rho - r_n)^2 - (\rho - R)^2}$$

$$y_t = \frac{r_n(\rho - R)}{\rho - r_n}$$

$$x_t = x_0 - \sqrt{r_n^2 - y_t^2}$$

r_n is the radius, and r_0 is the center of the spherical nose cap. And the apex point can be found from:

$$x_a = x_0 - r_n$$

f) Secant ogive: According to shape 4-f, this shape of stern is also formed by a segment of a circle, but the base of the shape is not on the radius of the circle defined by the ogive radius. The cylinder body will not be tangent to the curve of the stern at its base. The ogive radius ρ is not determined by R and L (as it is for a tangent ogive), but rather is one of the factors to be chosen to define the stern shape. If the chosen ogive radius of a secant ogive is greater than the ogive radius of a tangent ogive with the same R and L , then the resulting secant ogive appears as a tangent ogive with a portion of the base truncated.

$$\rho > \frac{R^2 + L^2}{2R} \quad \alpha = \arctan \frac{R}{L} - \arccos \frac{\sqrt{L^2 + R^2}}{2\rho}$$

Then the radius y at any point x as x varies from 0 to L is

$$y = \sqrt{\rho^2 - (\rho \cos \alpha - x)^2} + \rho \sin \alpha$$

g) Elliptical: According to Fig.4-g, this shape of the stern is one-half of an ellipse, with the major axis being the centerline and the minor axis being the base of the stern. A rotation of a full ellipse about its major axis is called a prolate spheroid, so an elliptical stern shape would properly be known as a prolate hemispheroid. This is not a shape normally found in usual submarines. If R equals L , this is a hemisphere.

$$y = R \sqrt{1 - \frac{x^2}{L^2}}$$

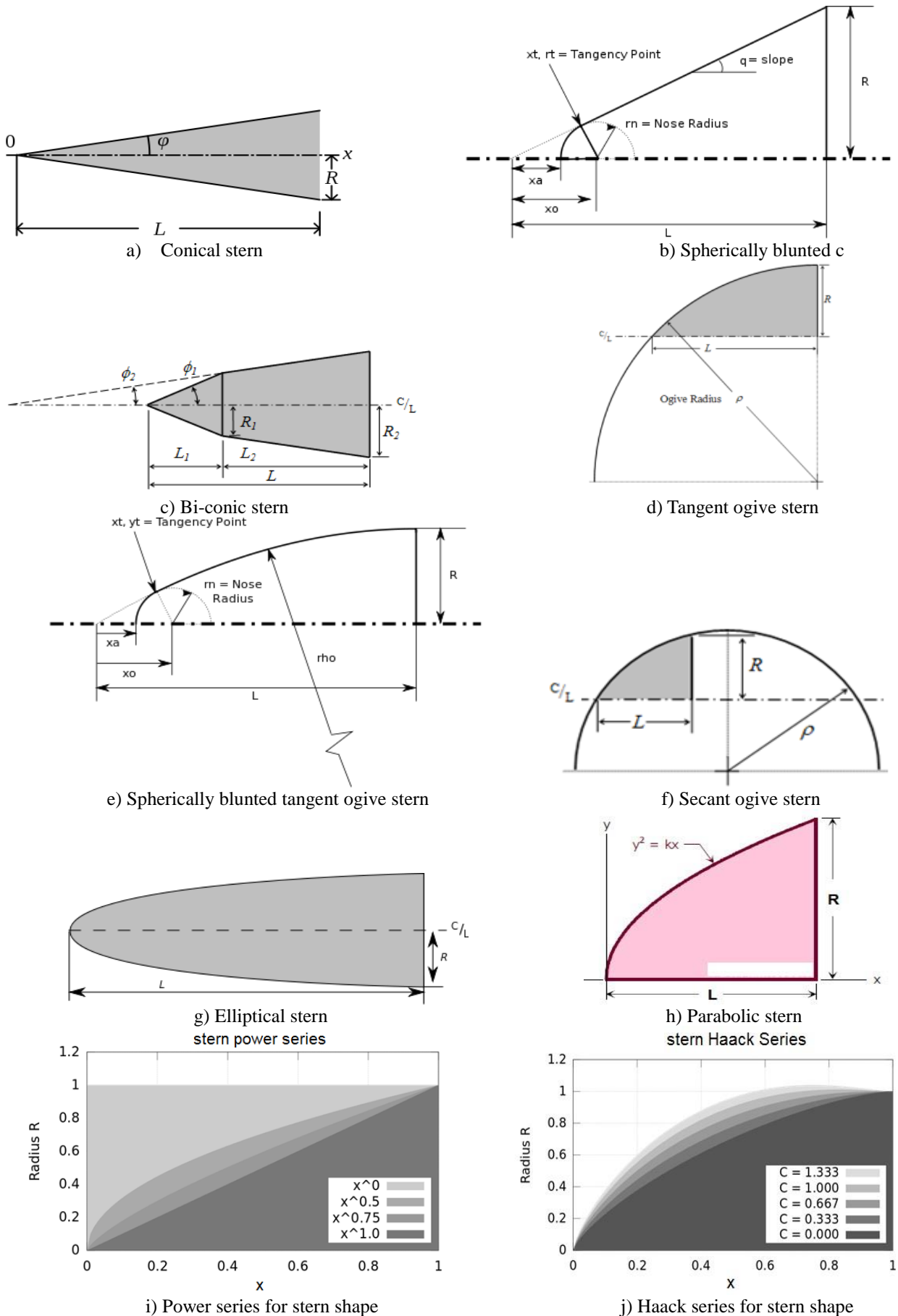


Fig. 4 Several shapes of stern [26,27]

h) Parabolic: This stern shape is not the blunt shape. The parabolic series shape is generated by rotating a segment of a parabola around an axis. This construction is similar to that of the tangent ogive, except that a parabola is the defining shape rather than a circle. Just as it does on an ogive, this construction produces a stern shape with a sharp tip (Fig.4-h).

$$\text{For } 0 \leq K' \leq 1: \quad y = R \frac{2 \frac{x}{L} - K' \left(\frac{x}{L}\right)^2}{2 - K'}$$

K' can vary anywhere between 0 and 1, but the most common values used for stern shapes are: $K'=0$ for a cone, $K'=0.5$ for a 1/2 parabola, $K'=0.75$ for a 3/4 parabola, $K'=1$ for a full parabola. For the case of the full Parabola ($K'=1$) the shape is tangent to the body at its base, and the base is on the axis of the parabola. Values of K' less than one, result in a slimmer shape, whose appearance is similar to that of the secant ogive. The shape is no longer tangent at the base, and the base is parallel to, but offset from, the axis of the parabola.

i) Power series: According to Fig.4-i, the power series includes the shape commonly referred to as a "parabolic" stern, but the shape correctly known as a parabolic stern is a member of the parabolic series (described above). The power series shape is characterized by its (usually) blunt tip, and by the fact that its base is not tangent to the body tube. There is always a discontinuity at the joint between stern and body that looks distinctly non-hydrodynamic. The shape can be modified at the base to smooth out this discontinuity. Both a flat-faced cylinder and a cone are shapes that are members of the power series. The power series stern shape is generated by rotating the $y = R(x/L)^n$ curve about the x -axis for values of n less than 1. The factor n controls the bluntness of the shape. For values of n above about 0.7, the tip is fairly sharp. As n decreases towards zero, the power series stern shape becomes increasingly blunt. Then for n , it can be said: $n=1$ for a cone, $n=0.75$ for a 3/4 power, $n=0.5$ for a 1/2 power (parabola), $n=0$ for a cylinder.

$$0 \leq n \leq 1: \quad y = R \left(\frac{x}{L}\right)^n$$

j) Haack series: despite of all the stern shapes above, the Haack Series shapes are not constructed from geometric figures. The shapes are instead mathematically

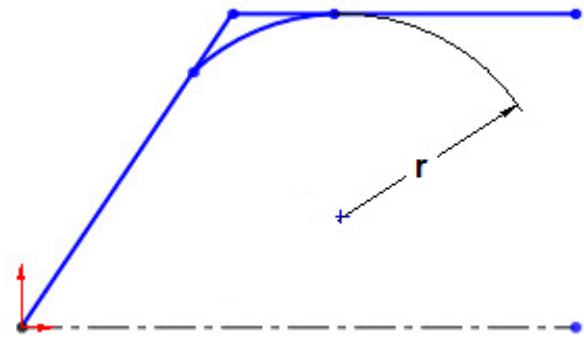


Fig. 5 Patched circle in discontinuity area of connection

derived for minimizing resistance. While the series is a continuous set of shapes determined by the value of C in the equations below, two values of C have particular significance: when $C=0$, the notation LD signifies minimum drag for the given length and diameter, and when $C=1/3$, LV indicates minimum resistance for a given length and volume. The Haack series shapes are not perfectly tangent to the body at their base, except for a case where $C=2/3$. However, the discontinuity is usually so slight as to be imperceptible. For $C > 2/3$, Haack stern bulge to a maximum diameter greater than the base diameter. Haack nose tips do not come to a sharp point, but are slightly rounded (Fig.4-j).

$$\theta = \arccos \left(1 - \frac{2x}{L} \right)$$

$$y = \frac{R}{\sqrt{\pi}} \sqrt{\theta - \frac{\sin 2\theta}{2}} + c \sin^3 \theta$$

Where: $C=1/3$ for LV-Haack and $C=0$ for LD-Haack.

k) Von Karman: The Haack series giving minimum drag for the given length and diameter, LD-Haack, is commonly referred to as the Von Karman or the Von Karman Ogive.

Patched Circle: In some cases which the connection between the cylinder and stern isn't fair with the sharp edge, a patched circle is used (Fig. 5). The discontinuity at the joint between stern and cylinder body, looks strongly non-hydrodynamic that should be cured by a patched circle. This circle is tangent to both cylinder and stern.

ASSUMPTIONS FOR THE MODELS

The base model that considered here, is an axis-symmetric body similar to torpedo, without any appendages because in this study, only stern effect on resistance, wants to be studied. It helps to quarterly CFD

Table 1 Main assumptions of models

| V (m/s) | L_t (m) | L_f (m) | L_m (m) | L (m) | D (m) | L/D | stern shape |
|------------|--------------|--------------|--------------|----------|----------|-------|--------------------------------------|
| 3 | 8 | 2 | 1 | 5 | 1 | 8 | Axis-symmetric without appendages |

Table 2 specifications of 14 models

| MODEL | specification of stern | A0 (m ²) | Aw (m ²) | V (m ³) |
|-----------|-------------------------------|-------------------------|-------------------------|---------------------|
| model 1-1 | simple conic | 3.14 | 16.1 | 3.14 |
| model 1-2 | conic with cut end | 3.14 | 17.69 | 3.46 |
| model 1-3 | Spherically blunted cone | 3.14 | 17.53 | 3.43 |
| model 2 | Bi-conic | 3.14 | 18.46 | 3.77 |
| model 3-1 | Tangent ogive | 3.14 | 18.74 | 3.93 |
| model 3-2 | Spherically blunted ogive | 3.14 | 19.6 | 4.13 |
| model 4 | ogive - concave circle | 3.14 | 13.48 | 2.61 |
| model 5 | elliptical | 3.14 | 20.6 | 4.45 |
| model 6-1 | parabolic with $k' = 0.5$ | 3.14 | 16.97 | 3.37 |
| model 6-2 | parabolic with $k' = 0.75$ | 3.14 | 17.67 | 3.58 |
| model 7-1 | power series - $n = 0.5$ | 3.14 | 18.71 | 3.8 |
| model 7-2 | power series - $n = 0.75$ | 3.14 | 17.22 | 3.4 |
| model 8-1 | Haack series with $c = 0$ | 3.14 | 18.47 | 3.8 |
| model 8-2 | Haack series with $c = 0.333$ | 3.14 | 19.24 | 4.04 |

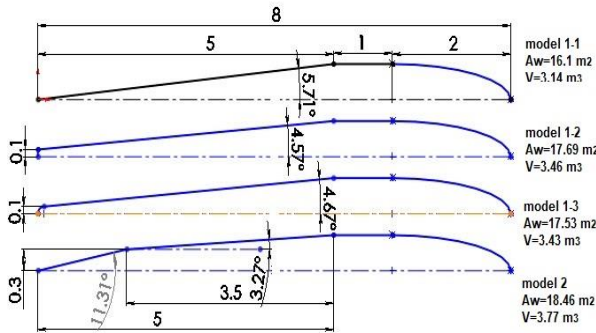


Fig. 6 Simple sterns without curvature

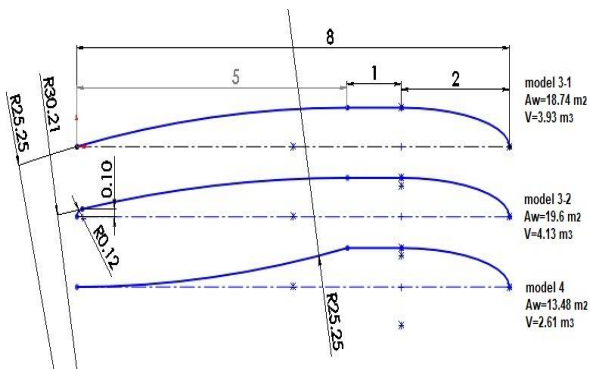


Fig. 7 Sterns that is formed by an ogive of circle

modeling of the body and saving the time. The bow is elliptical and middle part is a cylinder but stern part is different. In this paper, 14 models are studied. The 3D models and its properties are modeled in Solid Works. There are three main assumptions:

Assumptions 1: For evaluating the hydrodynamic effects of stern, the length of stern is unusually supposed large. It helps that the effects of stern be more visible.

Assumptions 2: The shape of bow and middle part are constant in all models. Bow shape is an elliptical shape and middle shape is cylindrical shape.

Assumptions 3: For providing more equal hydrodynamic conditions, the total length, bow, middle and stern lengths are constant. The diameter is constant too. Thus, L/D is constant in all models. These constant parameters, provide equal form resistance with except the stern shape and then the effects of stern shape, can be studied. Therefore, every model has different volume and wetted surface area.

The specifications of all 14 models are presented in Table 2. In addition, for CFD modeling in all models, velocity is constant and equal to 3 m/s. This velocity is selected so that the Reynolds number be more than five millions because M. Moonesun, in ref.[9] it was proved that total resistance coefficient after Reynolds of five millions remains constant.

According to Fig.6, model 1-1 is the simplest stern shape that is supposed the base model for comparison to the results of other models for optimization. In most submarines, the stern is blunted cone because of shaft exit. Models 1-2 and 1-3 show two categories for this kind of blunting. The diameter of the blunting is depended on the shaft diameter and bearing thickness at the location of end part. Therefore, this diameter is small compare to the hull diameter. Model 2 in Fig.6 shows a bi-conic stern that contains two cones with different slopes. Usually the slope angle of first cone is bigger than the slope of second cone because the main reason of this arrangement is providing more space in the end part of submarine; inside the pressure hull or inside the light hull as showed in Fig.2. Usually, ordinary and small submarines have bi-conic arrangement in stern. Fig.6 shows the stern shapes without curvature that are cheap and easy to construction, especially for small submarines and ROVs and AUVs.

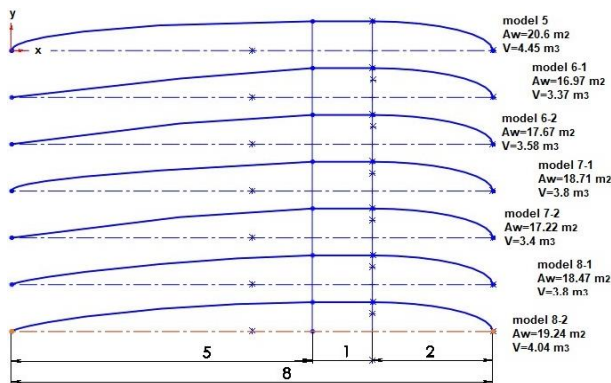


Fig. 8 Stems with functional curvature according to the equations of the sections g-k.

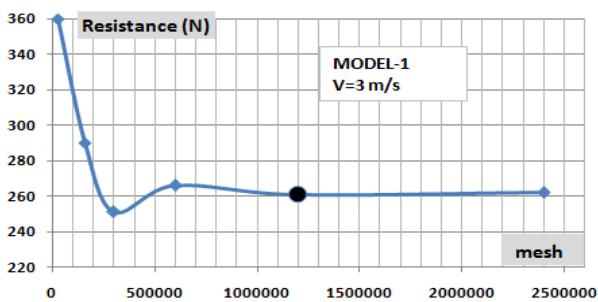


Fig. 9 Mesh independency evaluations

Fig.7 shows the stems which are formed by an ogive of a circle. These shapes are almost easy to construction because the curvature of a circle in comparison to the other curvatures in Fig.7 is simpler. Model 3-1 is ideal tangent ogive with the radius of 25.25 meters. The radius of this circle must be so big that the ogive can be tangent to the cylinder part. For exit the shaft, Model 3-2 is more applicable that is a Spherically blunted tangent ogive. This model is formed by two ogives: one large ogive with radius of 30.21 meters and one small ogive with the radius of 0.12 meters for blunting the main ogive. Model 4 is formed by a concave ogive and hollow shape, that is rarely applicable. This shape is an unusual shape and is mentioned here, only for scientific comparison of the results of the concave and convex ogive. In Fig.8, stems with functional curvature are shown. All equations of these shapes are presented in the sections g-k. The construction of these models is usually complicated, complex, expensive and time consuming. Utilization of these forms is only affordable, if considerable hydrodynamic advantages could be earned. This paper wants to answer to this question. In the types that stern include pressure and light hull, forming the pressure hull according to these equations are very difficult because

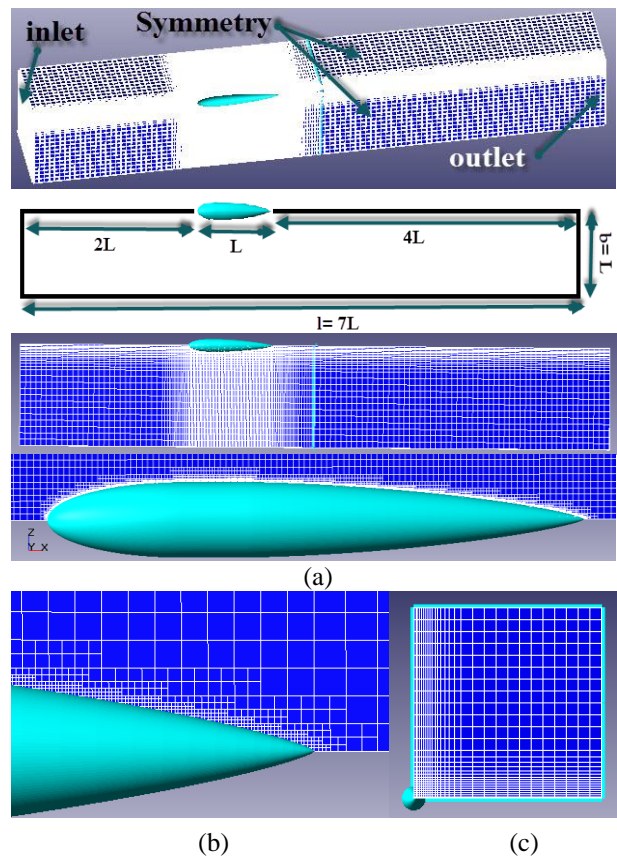


Fig. 10 (a) Domain and structured grid (b) Very tiny cells near the wall for boundary layer modeling and keeping y^+ about 30 (c) Quarterly modeling because of axis-symmetry

the thickness of the shell of pressure hull is very much. Therefore, only light hull can be formed by these functions. Model 5 is an elliptical shape that provides more volume in stern part of submarine but isn't so usual in design. Models 6-1 and 6-2 are parabolic shapes for $k = 0.5$ and 0.75 . Models 7-1 and 7-2 are according to the power series for $n = 0.5$ and 0.75 . Models 8-1 and 8-2 are according to Haack series for $n = 0$ and 0.333 .

There is a very little different between some of these models that can't be recognized with eyes such as Model 6-1 with Model 6-2. The wetted surface area and volume of each model is different to other models that these values are written beside the models.

CFD METHOD OF STUDY

This analysis is done by Flow Vision (V.2.3) software based on CFD method and solving the RANS equations. Generally, the validity of the results of this software has been done by several experimental test cases, and nowadays this software is accepted as a practicable and reliable

Table 3 Settings of the simulation

| Elements | Boundary conditions | Descriptions |
|------------|---------------------|--|
| Domain | Box | conditions Fully submerged modeling (without free surface)- quarter modeling- domain with inlet, outlet, symmetry and wall- Without heat transfer. |
| | | dimensions 56*8*8 m- length before and after model=16 & 32 m |
| | | grid structured grid- hexahedral cells- tiny cell near wall- Meshes more than 1.5 millions. |
| | | settings Iterations more that 1500- Time step = 0.01sec. |
| Fluid | - | Incompressible fluid- Reynolds number more than 24 millions- turbulent modeling: Standard k- ϵ - fresh water- tempreture: 20 deg- $\rho = 999.841 \text{ kg/m}^3$. |
| Object | Wall | Bare hull of submarine- value $30 < y+ < 100$ - roughness = 0- no slip |
| Input | Inlet | Velocity = 3m/s- constant- normal (along x)- in 1 face |
| Output | Free outlet | Zero pressure- in 1 face |
| Boundaries | Symmetry | In 4 faces |

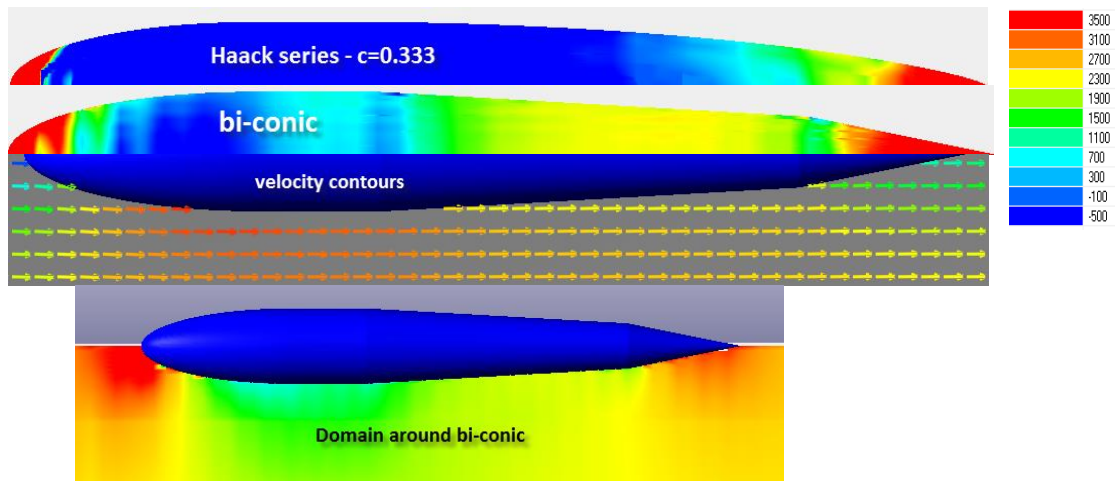


Fig. 11 pressure contour around the body

software in CFD activities. For modeling these cases in this paper, Finite Volume Method (FVM) is used. A structured mesh with cubic cell has been used to map the space around the submarine. For modeling the boundary layer near the solid surfaces, the selected cell near the object is tiny and very small compared to the other parts of domain.

For selecting the proper quantity of the cells, for one certain model (Model1) and $v = 3\text{m/s}$, six different amount of meshes were selected and the results were compared insofar as the results remained almost constant after 1.2 millions meshes, and it shows that the results are independent of meshing (Fig.9). In all modeling the mesh numbers are considered more than 1.8 millions.

For the selection of suitable iteration, it was continued until the results were almost constant with variations less than one percent, which shows the convergence of the solution. All iterations are continued to more than one millions.

In this domain, there is inlet (with uniform flow), Free outlet, Symmetry (in the four faces of the box) and Wall (for the body of submarine). Dimensions of cubic domain are 56m length (equal to 7L), 8m beam and 8m height (equal to L or 8D). Pay attention to that only quarter of the body is modeled because of axis-symmetric shape, and the domain is for that. Meanwhile, the study has shown that the beam and height equal to 8D in this study can be acceptable. Here, there are little meshes in far from the object. The forward distance of

the model is equal to 2L and after distance is 4L in the total length of 7L (Fig. 10). The turbulence model is K-Epsilon, turbulent scale is considered 0.1m and y^+ is considered 30~100. The considered flow is incompressible fluid (fresh water) in 20 degrees centigrade and constant velocity of 3 m/s. Time step of each iteration, depends on the model length and velocity so here, time step is defined equal to 0.01 second i.e. the full model length is traversed at 2.67 second or 267 iterations. It is minimum number of iterations. In this paper, all models are performed by more than 1500 iterations. Settings of the simulation are collected in Table 3.

CFD RESULTS ANALYSIS

CFD analyses for all 14 models were done by Flow Vision software under the conditions that were mentioned above. All results are for fully submerged condition without free surface effects. Pressure distribution with viscosity effects, results in total resistance. Therefore, total resistance is the summation of pressure (form) resistance and viscous (frictional) resistance. Pressure contours around the body are shown in Fig. 11 for sample for Model 3-1. Fore part of the object includes stagnation point and high pressure area. Middle part is low pressure area, but stern part is high pressure area. Non-uniform distribution of pressure on the body, results in pressure resistance. If the stern design be a stream lined form, the high pressure area in aft part is reduced and results in lower pressure resistance. In the other words, the better stern design, means the lesser pressure in stern part.

In viscous resistance, an important function is wetted area resistance. This parameter varies in all models, but cross section area is constant because the diameter is constant in all models. The amount of area was presented in Tab.2 and for better comparison, it was presented in the diagram of Fig.12. Concave ogive shape (Model 4) results minimum and elliptical shape (Model 5) results in the maximum wetted area. Base on the area, two kinds of the resistance coefficient can be defined: 1-based on wetted area: $C_{d1} = R/0.5\rho A v^2$ that is usually used for the frictional resistance coefficient. 2-based on cross section area: $C_{d0} = R/0.5\rho A_0 v^2$ that is usually used for the pressure resistance coefficient. Here, for accounting the effect of the wetted area on the coefficients, all coefficients are presented as a function of the wetted area.

Table 4 Resistances and Coefficients for 14 models

| MODEL | Rt | Rp | Rv | Ct*1000 | Cp*1000 | Cv*1000 |
|-----------|-------|------|-------|---------|---------|---------|
| Model 1-1 | 262 | 54.4 | 207.6 | 3.616 | 0.75086 | 2.865 |
| Model 1-2 | 290.4 | 60.8 | 229.6 | 3.648 | 0.76377 | 2.884 |
| Model 1-3 | 288.8 | 63.6 | 225.2 | 3.661 | 0.80624 | 2.855 |
| Model 2 | 300.8 | 65.6 | 235.2 | 3.621 | 0.78970 | 2.831 |
| Model 3-1 | 298.8 | 60.4 | 238.4 | 3.543 | 0.71623 | 2.827 |
| Model 3-2 | 302 | 62 | 240 | 3.424 | 0.70295 | 2.721 |
| Model 4 | 226.4 | 49.6 | 176.8 | 3.732 | 0.81767 | 2.915 |
| Model 5 | 341.2 | 84.8 | 256.4 | 3.681 | 0.91478 | 2.766 |
| Model 6-1 | 280 | 59.2 | 220.8 | 3.667 | 0.77522 | 2.891 |
| Model 6-2 | 291.2 | 61.2 | 230 | 3.662 | 0.76967 | 2.893 |
| Model 7-1 | 269.6 | 32 | 237.6 | 3.202 | 0.38007 | 2.822 |
| Model 7-2 | 280.8 | 58.8 | 222 | 3.624 | 0.75881 | 2.865 |
| Model 8-1 | 292.8 | 58.8 | 234 | 3.523 | 0.70745 | 2.815 |
| Model 8-2 | 275.6 | 32.4 | 243.2 | 3.183 | 0.37422 | 2.809 |

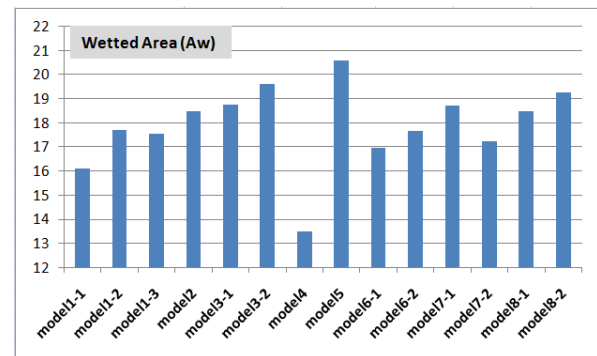


Fig. 12 wetted area comparison in 14 models

The amount of total resistance, pressure resistance and viscous resistance and their coefficients are presented in Tab. 4. For better comparison, the diagrams of total resistance (Fig. 13-a), pressure resistance (Fig. 13-b), total resistance coefficient (Fig.13-c) and pressure resistance coefficient (Fig.13-d) are presented.

In total resistance, wetted area coefficient is important, therefore, according to Fig.12 and 13-a, the Model 4 has minimum and Model 5 has maximum resistance. Pressure resistance is a function of form efficiency. If the shape has stream lined form without discontinuity and breaking, the pressure resistance will be minimum. In this study, an ideal stern form should have minimum resistance. It should be remembered that two main parameters there are here: 1-wetted area which affects the frictional resis-

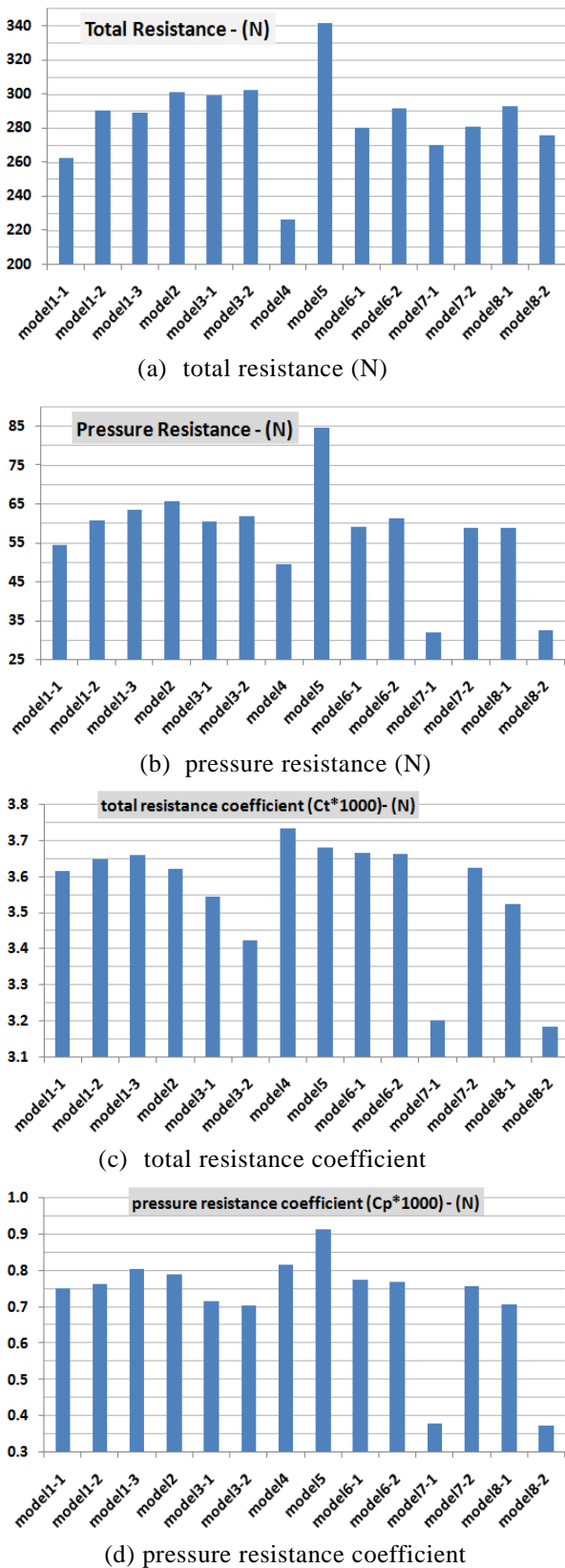


Fig. 13 Resistances and Coefficients for 14 models

tance 2-general form which affects the pressure resistance by better distribution of pressure on the body and avoiding low pressure area in the aft part of the body.

Fig.13-b shows the pressure resistance diagrams that Model 7-1 (power series with $n = 0.5$) and Model 8-2 (Haack series with $c = 0.333$) have minimum pressure resistance but Model 5 (elliptical) has maximum amount. The trends of resistance coefficients are different and to some extent, amazing.

According to Fig.13-c, the total resistance coefficients of Model 7-1 (power series with $n = 0.5$) and Model 8-2 (Haack series with $c = 0.333$) have minimum but Model 4 (ogive-concave circle) has the the maximum amount. It means that, if the wetted area of all models be equal, Models 7-1 and 8-2 are the best designs and the Model 4 is the worse design. Here the role of the wetted area is considerable. In Ogive with concave circle (concave ogive) shape, it was shown that, it has minimum total resistance but since its wetted area was minimum, then the total resistance coefficient was maximum. It is an amazing note in hydrodynamic design.

Diagrams in Fig.13-d show that another time, Model 7-1 (power series with $n = 0.5$) and Model 8-2 (Haack series with $c = 0.333$) has minimum but Model 5 (elliptical stern) has a maximum pressure resistance coefficient. It means that, in form design aspect of view, Models 7-1 and 8-2 are the best designs, and the Model 4 is the worse design. Here the role of curvature and pressure distribution on the curvature is considerable.

In some cases, providing a large volume for accommodating the MBT tanks or other devices inside the stern is important. Here, the criterion is providing more space and bigger volume. According to Tab.2 and Figs.13a and 13b, for a constant volume, it seems that elliptical stern (Model 5) be a bad design because of the high resistance result, but spherically blunted ogive (Model 3-2) be a better choice.

CONCLUSION

In conclusion, the results of this study can be said as:

1. The hydrodynamic design of stern is important, but the results show that, its importance isn't comparable with the importance of the bow of submarine. This comparison can be done by Ref.[20]. It seems that the hydrodynamic importance of the stern is not in resistance values but on the wake field. The quality of the inlet flow to the propeller will be shown in wake factor with considerable hydrodynamic consequences.

2. If the wetted area of all models be equal, stern shape with power series with $n = 0.5$ and Haack series with $c = 0.333$ are the best designs and the ogive-concave circle is the worse design (from Fig.13-c).
3. If the volume of all models be equal, it seems that elliptical stern be a bad design because of the high resistance results, but spherically blunted ogive be a better choice (from Tab. 2 and Figs.13a and 13b).
4. If the stern length of all models be equal, stern shape of the concave ogive is the best design, and the elliptical stern is the worse design (from Fig.13-a). In practical point of view, Neither concave ogive, nor elliptical stern aren't so common practice. After that, it can be advised that, simple conic with any curvature is the best selection and three shapes of bi-conic, Tangent ogive, Spherically blunted ogive are the worse design. In real design of submarines, usually, the stern length supposes be constant, therefore, a simple conic shape of stern is a good advise with good hydrodynamic results, easy to construction and low in cost. It is the most important earning of this paper.

NOMENCLATURE

| | |
|--|---|
| L_t | total length of submarine (m) |
| L | stern length of submarine (m) |
| L_m | middle part length of submarine (m) |
| L_f | fore (bow) length of submarine (m) |
| D | diameter of the cylinder part (or) radius of the base of the stern |
| x | variable along the length. x varies from 0 to L |
| y | is the radius at any point of the x |
| C_t | total resistance coefficient is shown in *1000 |
| C_p | pressure resistance coefficient is shown in *1000 |
| C_v | viscous resistance coefficient is shown in *1000 |
| φ | half angle of stern cone |
| IHSS | Iranian Hydrodynamic Series of Submarines |
| A_0 | cross section area ($3.14 * D^2 / 4$) in m^2 |
| A_w | wetted area (outer area subject to the water) in m^2 |
| MBT | Main Ballast Tank for providing reserve of buoyancy and ability to surfacing of submarine |
| V | total volume of submarine in m^3 |
| v | speed of submarine in m/s |
| R_t | Total resistance |
| R_p | pressure resistance |
| R_v | viscous resistance |
| * Other parameters are described inside the text | |

REFERENCES

1. Moonesun, M., P. Charmdooz, "General arrangement and naval architecture aspects in midget submarines," 4th International Conference on Underwater System Technology Theory and Applications (USYS'12), Malaysia (2012).
2. Iranian Defense Standard (IDS-857), *Hydrodynamics of Medium Size Submarines* (2011)
3. Mackay, M, "The Standard Submarine Model: A Survey of Static Hydrodynamic Experiments and Semiempirical Predictions" Defence R&D Canada (2003).
4. Jackson, H A, "Submarine Design Notes," Massachusett Institute of Technology, pp.520 (1982).
5. Burcher, R, L.J. Rydill, "Concept in Submarine Design," The Press Syndicate of the University of Cambridge, Cambridge University Press, pp.295 (1998).
6. A Group of Authorities, *Submersible Vehicle System Design*, The Society of Naval Architects and Marine Engineers (1990).
7. Gabler, Ulrich, *Submarine Design*, Bernard & Graefe Verlag (2000).
8. Kormilitsin, Y.N., O.A. Khalizev, *Theory of Submarine Design*, Saint-Petersburg State Maritime Technology University, 2001
9. Greiner, L., *Underwater Missile Propulsion: a Selection of Authoritative Technical and Descriptive Papers*, Compass Publications, USA (1968).
10. Joubert, P.N., "Some Aspects of Submarine Design: part 1: Hydrodynamics," Australian Department of Defence (2004).
11. Joubert, P.N., "Some Aspects of Submarine Design: part 2: Shape of a Submarine 2026," Australian Department of Defence (2004).
12. Moonesun, M., M. Javadi, P. Charmdooz, U.M. Korol, "Evaluation of Submarine Model Test in towing Tank and Comparison with CFD and Experimental Formulas for Fully Submerged Resistance," *Indian Journal of Geo-Marine Science*, Vol.42(8), pp.1049-1056 (2013).
13. Roddy, R., "Investigation of the Stability and Control Characteristics of Several Configurations of the DARPA SUBOFF Model (DTRC Model 5470) from Captive-Model Experiments," Report No. DTRC/SHD-1298-08, (1990).
14. Moonesun, M., U.M. Korol, V.O. Nikrasov, S. Ardeshiri, D. Tahvildarzade, "Proposing New Criteria for Submarine Seakeeping Evaluation," 15th Marine Industries Conference (MIC2013), Kish Island (2013).

15. Timothy, Presterio, "Verification of a Six-Degree of Freedom Simulation Model for the REMUS Autonomous Underwater Vehicle," University of California at Davis (1994).
16. Praveen, P.C., P. Krishnankutty, "Study on the Effect of Body Length on Hydrodynamic Performance of an Axis-Symmetric Underwater Vehicle," *Indian Journal of Geo-Marine Science*, Vol.42(8), pp.1013-1022 (2013).
17. Suman, K.N.S., D. Nageswara Rao, H.N. Das, G. Bhanu Kiran, "Hydrodynamic Performance Evaluation of an Ellipsoidal Nose for High Speed Underwater Vehicle," *Jordan Journal of Mechanical and Industrial Engineering (JJMIE)*, Vol.4, pp. 641-652 (2010).
18. Stenars, J.K., *Comparative Naval Architecture of Modern Foreign Submarines*, Massachusetts Institute (1988).
19. Moonesun, M., Y.M. Korol, D. Tahvildarzade, M. Javadi, "Practical Solution for Underwater Hydrodynamic Model Test of Submarine," *Journal of the Korean Society of Marine Engineering* (under publishing) (2014).
20. Moonesun, M., Y.M. Korol, "Concepts in Submarine Shape Design," 16th Marine Industries Conference (MIC2013), Bandar Abbas, Iran (2013).
21. Budiyono, A, "Advances in Unmanned Underwater Vehicles Technologies: Modeling, Control and Guidance Perspectives," *Indian Journal of Marine Science*, Vol.38 (3), pp.282-295 (2009).
22. Lee, J.M., J.Y. Park, B. Kim, H. Baek, "Development of an Autonomous Underwater Vehicle IsiMI6000 for Deep Sea Observation," *Indian Journal of Geo-Marine Science*, Vol.42 (8), pp.1034-1041 (2013).
23. Minnick, Lisa, "A Parametric Model for Predicting Submarine Dynamic Stability in Early Stage Design," Virginia Polytechnic Institute and State University (2006).
24. Alemayehu, D., R.B. Boyle, E. Eaton, T. Lynch, J. Stepanchick, R. Yon, "Guided Missile Submarine SSG(X)," SSG(X) Variant 2-44, Ocean Engineering Design Project, AOE 4065/4066, Virginia Tech Team 3 (2006).
25. Moonesun, M., "Introduction of Iranian Hydrodynamic Series of Submarines (IHSS)," *Journal of Taiwan Society of Naval Architects and Marine Engineers*, ISSN 1023-4535, Vol.33, No.3, pp.155-162 (2014).
26. www.en.wikipedia.org/ the free encyclopedia
27. Bronshtein, I.N., K.A. Semendyayev, Gerhard Musiol, Heiner Mühlig, *Handbook of Mathematics*, ISBN-13: 978-3540721215 (2007)

(Manuscript received Jul. 27, 2014,
Accepted for publication Oct. 27, 2014)